Ferromagnetic resonance studies of accumulation and diffusion of spin momentum density in Fe/Ag/Fe/GaAs(001) and Ag/Fe/GaAs(001) structures

B. Kardasz* and B. Heinrich

Physics Department, Simon Fraser University, 8888 University Drive, Burnaby, British Columbia, Canada V5A 1S6

(Received 17 November 2009; revised manuscript received 8 February 2010; published 8 March 2010)

Spin transport was investigated in magnetic single GaAs/16 Fe/*m*Ag/20 Au(001) and double GaAs/16 Fe/*n*Ag/12 Fe/20 Au(001) layer structures prepared by molecular-beam epitaxy, where $m=0,5,20,1500$ and $n=20,100,300,500,1500$. The integers represent the number of Fe, Ag, and Au atomic layers, respectively. The set of Ag spacers in magnetic double layers allowed one to investigate nonlocal spin transport from ballistic to fully developed spin-diffusion limit. The spin transport in these structures was investigated using spin pumping effect at the 16Fe/Ag(001) interface. Ferromagnetic resonance (FMR) studies were carried out using standard microwave spectrometers at 9, 36, and 72 GHz. The FMR linewidth ΔH in the above structures was found to follow Gilbert damping mechanism. The measured ΔH as a function of the Ag spacer thickness in GaAs/16 Fe/*n* Ag/12 Fe/20 Au(001) was interpreted using Kirchhoff's laws for spin electronics which includes the spin diffusion across the Ag spacer allowing one to determine the electron charge and spin-flip time scattering parameters and the spin-diffusion length in the Ag thin-film spacers.

DOI: 10.1103/PhysRevB.81.094409 PACS number(s): 72.25.−b, 72.15.Lh, 75.70.−i, 76.50.+g

I. INTRODUCTION

Spin dynamics and spintronic devices are increasingly based on nonlocal spin transport using magnetic films where spin-dependent electron scattering plays a significant role; see, e.g., lateral spin valves[1–3] and spin Hall effects.[4] In these systems the accumulated spin-density in a normal-metal (NM) polycrystalline thin-film wire is generated by a partially spin polarized electric current at the ferromagnetic/normal-metal (F/NM) interface. A quantitative description of spin transport in these systems is complicated by grain boundaries in polycrystalline NM wires and complex structure of F/NM and NM/F junctions. The studies presented in this paper were carried out by investigating the spin transport in crystalline Ag films in magnetic single Fe/Ag and double Fe/Ag/Fe thin-film structures by injecting a pure spin current at the Fe/Ag interface using rf spin-pumping effect. This simplifies the quantitative treatment of spin injection and avoids electron scattering at polycrystalline grains. However the interface electron diffuse scattering was present in our samples. It will be shown that its presence is a necessary prerequisite for the quantitative treatment of spin transport in thin magnetic heterostructures with a weak electron-phonon scattering. The data analysis was carried out using Kirchhoff's laws of spintronics.[5] The Ag spacers with the *n* atomic layers ($n=20,100,300,500,1500$) in Fe/Ag/Fe structures allowed one to investigate nonlocal spin transport from ballistic to fully developed spin-diffusion limit.

The planar thin-film geometry used in this paper is similar to those employed in the current-perpendicular-to-plane giant magneto resistance (CPP-GMR) structures and magnetic tunneling junction (MTJ) devices.

The intrinsic ferromagnetic resonance (FMR) linewidth ΔH (half width at half maximum) in the measured Fe films was found to be linearly dependent on the effective microwave angular frequency field ω/γ, where γ is absolute value of gyromagnetic ratio. The coefficient of proportionality is given by the dimensionless Gilbert damping parameter α, $\Delta H=\alpha(\omega/\gamma)$. In magnetic multilayer which include ferromagnetic and normal-metal spacer layers one has to include interface spin pumping.[6,7] Spin dynamics generates a peristaltic interface spin current at the F/NM interface leading to an accumulated spin density in NM. This accumulated density diffuses across the NM spacer and leads to interface damping. The itinerant electrons in normal metal are affected by momentum, τ_m, (leading to electrical resistance) and spin-flip, τ_{sf}, (leading to loss of spin momentum) scattering parameters. In normal metals the spin-flip scattering is caused by weak spin-orbit coupling. This means that only some of the momentum scattering events are accompanied by spin-flip events, and therefore $\tau_{sf} \gg \tau_m$, see Ref. 8. The spin-diffusion length $\delta_{sd}=v_F(\tau_m\tau_{sf}/3)^{1/2}$ represents the length scale on which the accumulated momentum density in NM relaxes back to the lattice.

The results presented in this paper are an extension of our studies of spin transport in the Au films using Fe/Au(001) and Fe/Au/Fe(001) structures.[9,10]

II. GROWTH STUDIES

The Fe, Ag, and Au films were deposited at room temperature (RT) under ultrahigh vacuum (UHV) conditions ($\simeq 10^{-10}$ Torr pressure) using molecular-beam epitaxy (MBE). The substrate was a commonly used 4×6-GaAs(001) reconstructed template. The 4×6 surface reconstruction was obtained by subsequent atomic hydrogen cleaning, Ar^+ sputtering and annealing the GaAs(001) wafer at $\simeq 600$ °C. Reflection high-energy electron diffraction (RHEED) patterns and scanning tunneling microscopy (STM) images showed that this reconstruction consists of two mixed phases: (a) ~95% is 2×6 reconstruction having As dimers and dangling bonds oriented along the $[1\bar{1}0]$ crystallographic direction. (b) ~5% is 4×2 GaAs(001) with the dangling bonds of Ga oriented along the [110] direction.

Layer-by-layer growth was monitored by means of RHEED intensity oscillations. After deposition of an equiva-

lent of three atomic layers of Fe on GaAs(001) a continuous film was formed. The surface of Fe and Ag films consisted of atomic terraces approximately 3–4 and 15 nm wide, respectively. All studied structures were terminated by a crystalline 20 Au(001) layer for protection in ambient conditions. Further details can be found in Ref. 10. The following single and double layer magnetic structures were prepared: GaAs/16 Fe/mAg/20 Au(001) and GaAs/16 Fe/nAg/12 Fe/20 Au(001) (m=0,5,20, 1500 and n=20,100,300,500,1500). The integers represent the number of atomic layers. The spacing between the atomic layers are 0.145, 0.204, and 0.2045 nm for Fe, Au, and Ag, respectively.

The surface passivation by Au of the Ag surface in the Fe/Ag(001) samples was an essential step. The samples without the Au cap layer were quickly affected by a small level surface oxidation of Ag which led surprisingly to lattice defects in the underlying Fe film resulting in significant extrinsic magnetic damping (two magnon scattering) making the study of spin transport in uncapped GaAs/Fe/Ag samples impossible.

III. SPIN PUMPING THEORY

Quantitative description of spin transport in magnetic metallic heterostructures by magnetoelectronics and Kirchhoff's laws[11] employs a concept of accumulated spin density and spin current in NM. It is not *a priori* clear how Kirchhoff's laws can be applied to ultrathin NM layers where electrons can propagate between interfaces in ballistic manner. One needs a globally diffuse system where the momentum distribution of incident electrons on each interface is randomized and consequently one can define the chemical potential for the majority and minority electrons resulting in the accumulated density of spins in NM. Tserkovnyak *et al.*[5] showed that such randomization in the momentum space can be provided by a sufficient interface diffuse scattering. The interface scattering in GaAs/Fe/Au(001) structures was investigated in our quantitative in-plane GMR studies. The sheet resistances were measured as a function of the film thickness and the results were interpreted by using semiclassical Boltzmann equation which incorporates the electronic properties from first-principles local-density calculations.[12] The measured magnetoresistance was found to be consistent with the diffuse (random) scattering parameters P=0.45 and 0.23 for the minority and majority spins at the Fe/Au interface and nearly complete diffuse scattering (P=1) at the Au/vacuum interface. This means that even in MBE grown crystalline samples the diffuse scattering at interfaces is strongly present and thus allowing one to use the concept of spin electronic circuits and Kirchhoff's laws. Tserkovnyak *et al.*[5] showed that in this case the interface impedances (obtained from first-principles band calculations) have to be renormalized by subtracting from them the Sharvin impedance, see further discussion in Ref. 5.

In F1/NM/F2 and F/NM systems the circuit elements are as follows: (a) ferromagnetic layers provide spin current terminals; sources (spin pump) and sinks (spin detector). (b) F1/NM, NM/F2, and NM/vacuum (ambient) interfaces represent the circuit nodes. (c) NM spacer represents a spatially extended spin conductor.

The spin dynamics in the classical limit in a single ultrathin ferromagnetic film can be described by the Landau-Lifshitz-Gilbert (LLG) equation of motion[13]

$$\frac{1}{\gamma}\frac{\partial \boldsymbol{M}}{\partial t} = -[\boldsymbol{M}\times \boldsymbol{H}_{\mathrm{eff}}] + \frac{\alpha}{\gamma}\left[\boldsymbol{M}\times\frac{\partial \boldsymbol{u}}{\partial t}\right], \tag{1}$$

where $\boldsymbol{u}$ is the unit vector in the direction of the magnetization $\boldsymbol{M}$, $\gamma = g|e|/2mc$ is the absolute value of the gyromagnetic ratio, and α is the dimensionless Gilbert damping parameter. The first term on the right-hand side represents the precessional torque in the internal field $\boldsymbol{H}_{\mathrm{eff}}$ and the second term represents the Gilbert damping torque.[13,14] Tserkovnyak *et al.*[6] and Heinrich *et al.*[7] showed that an interface damping can be generated by pumping the spin current from a ferromagnet (F) into an adjacent normal-metal (NM) layer. The pumped spin momentum is given by

$$\boldsymbol{I}_{sp} = \frac{\hbar}{4\pi}\mathrm{Re}(g_{\uparrow\downarrow})\left[\boldsymbol{u}\times\frac{\partial \boldsymbol{u}}{\partial t}\right], \tag{2}$$

where $g_{\uparrow\downarrow}$ is the spin mixing conductance (in units of e^2/h) is dependent on the transmission $t^{\uparrow}, t^{\downarrow}$ and reflection $r^{\uparrow}, r^{\downarrow}$ coefficients for majority ($\uparrow$) and minority ($\downarrow$) spins, respectively;

$$g_{\uparrow\downarrow} = \sum_{l}[1 - \mathrm{Re}(r_l^{\uparrow}r_l^{\downarrow *} + t_l^{\uparrow}t_l^{\downarrow *})] \approx \frac{k_F^2}{4\pi} = 1.2n^{2/3}, \tag{3}$$

where l is the number of spin channels impinging at the F/NM interface, k_F is the wave-number at the Fermi surface of NM, and n is the density of electrons per spin in the normal-metal NM. For small precessional angles of $\boldsymbol{M}$ the pumped spin momentum is almost entirely transverse to the static magnetic moment. In magnetic Au/Fe/Ag/Fe/GaAs(001) double layer structures the FMR fields can be separated by several kOe due to the presence of strong interface anisotropies.[7,13] As it was pointed out above the spin mixing conductance $g_{\uparrow\downarrow}$ has to be replaced by its renormalized value by subtracting the Sharvin resistance,

$$\frac{1}{\tilde{g}_{\uparrow\downarrow}} = \frac{1}{g_{\uparrow\downarrow}} - \frac{1}{g_{sh}}. \tag{4}$$

The interface and Shavrin conductances for Fe/Au(001) interfaces were calculated by Zwierzycki *et al.*[15] using density-functional electron band calculations. The Shavrin conductance is half of the $g_{\uparrow\downarrow}=1.2\times10^{15}$ cm^{-2} in units of e^2/h. This means $\tilde{g}_{\uparrow\downarrow}=2g_{\uparrow\downarrow}$. The difference in $g_{\uparrow\downarrow}$ between the Au and Ag spacers is negligible because the densities of electrons in Ag and Au are almost identical [see Eq. (3)].

Our calculations were limited to spin-diffusion theory. In fact at the present time there is no spin transport theory equivalent to nonlocal net electron transport using Boltzmann's equations. The spin transport equations at the interfaces (nodes) are described by Tserkovnyak *et al.*[5] The spin current generated at the F1/NM interface leads to an accumulated spin momentum density $\boldsymbol{s}_N$ inside the NM spacer layer. At the F1/NM node the accumulated spin-density

partly flows back to the F1 spin reservoir. This back flow is given by Eq. (26) in Ref. 5. In our experiments we used a small rf excitation and consequently spin pumping leads to only transverse (with respect to the magnetic moment of F1) accumulated spin density [see Eq. (2)]. This significantly simplifies the spin back-flow current because its transverse component is entirely absorbed by F1 at the interface F1/NM. In the work by Tserkovnyak, Brataas, and Bauer the induced spin flow is expressed using the spin accumulation vector $\boldsymbol{\mu}_s=\boldsymbol{\mu}_\uparrow-\boldsymbol{\mu}_\downarrow$, where $\boldsymbol{\mu}_\uparrow$ and $\boldsymbol{\mu}_\downarrow$ are the Fermi levels for the majority and minority electrons in NM. This is not intuitive picture for experimentalists. In experiments one measures directly the flow of spin momentum which enters the right hand side of LLG equations of motion (1). Using a simple relationship $\mathbf{s}_N=(\hbar/2)N(E_F)\boldsymbol{\mu}_s$ between the accumulated spin density $\mathbf{s}_N$ and $\boldsymbol{\mu}_s$ and replacing the spin mixing conductance $g_{\uparrow\downarrow}$ by the number of impinging electron channels at the F/NM interface, see Eq. (3) one can show that that the back spin flow current in Eq. (26) in Ref. 5 is given by

$$-\frac{1}{2}v_F\boldsymbol{s}_N, \tag{5}$$

where v_F and $N(E_F)$ are the Fermi velocity in NM, and electron density of states at the Fermi level in NM, respectively. The fraction 1/2 represents an effective transmission coefficient between NM and F.

At this point one can write the full set of Kirchhoff's equations using the layer F1 as spin current source magnetic terminal and layer F2 as spin sink magnetic terminal. The F1/NM, NM/F2, and NM/vacuum interfaces are the circuit nodes and the NM spacer as a spatially distributed spin conductor.

F1/NM node: first and second Kirchhoff's laws for the terminal F1 and node F1/NM are included in equation,

$$\boldsymbol{j}_s-\frac{1}{2}v_F\boldsymbol{s}_N=-D\frac{\partial\boldsymbol{s}_N}{\partial x}, \tag{6}$$

where the spin current source $\boldsymbol{j}_s$ is given by Eq. (2) with $g_{\uparrow\downarrow}$ replaced by $\tilde{g}_{\uparrow\downarrow}$. The right-hand side represents the net flow of spin momentum from F1 into NM (continuity of the spin current at the F1/NM node) and D is the diffusion coefficient in NM given by

$$D=v_F^2\tau_m/3, \tag{7}$$

where τ_m is the electron momentum relaxation time. Notice that the terminal F1 acts also as a spin sink.

NM/F2 node: continuity of the current at the NM/F2 node. The F2 terminal acts as a spin sink,

$$-D\frac{\partial\boldsymbol{s}_N}{\partial x}=\frac{1}{2}v_F\boldsymbol{s}_N. \tag{8}$$

The boundary condition in Eq. (8) is valid for the case when the layer F2 is off resonance and therefore contributes negligibly to spin pumping. The magnetic momentum current reaching the NM/F2 interface is fully absorbed by the F2 layer (spin detector) and acts as a driving torque for the F2 layer resulting in its rf excitation, see Ref. 10.

NM/vacuum node: the second terminal is vacuum (ambient) that reflects the spin current,

$$\frac{\partial\boldsymbol{s}_N}{\partial x}=0. \tag{9}$$

The spin momentum transport across the NM spacer is described by diffusion equation (equivalent to distributed conductance)[5]

$$\frac{\partial\boldsymbol{s}_N}{\partial t}=D\frac{\partial^2\boldsymbol{s}_N}{\partial x^2}-\frac{1}{\tau_{sf}}\boldsymbol{s}_N, \tag{10}$$

where τ_{sf} is the spin-flip relaxation time and x is the coordinate in the perpendicular direction to the interface. Equation (10) determines the penetration of $\boldsymbol{s}_N$ inside the NM spacer. The spin-diffusion length in the limit of low driving frequencies ($\omega\ll 1/\tau_{sf}$) is given by

$$\delta_{sd}=(D\tau_{sf})^{1/2}=v_F(\tau_{sf}\tau_m/3)^{1/2}. \tag{11}$$

Solutions of differential Eq. (10) require two vectorial boundary conditions. For magnetic single F1/NM and double F1/NM/F2 layer structures they are given by Eqs. (6) and (9) and Eqs. (6) and (8), respectively. These equations are equivalent to Eqs. (65), (67), and (77) in Ref. 5.

The above diffusion equations can be solved analytically. The additional interface damping in F1 is given by the net spin-current flow at the F1/NM interface [see Eq. (6)]. For F1/NM structures this leads to the interface damping parameter α_{sp}

$$\alpha_{sp}^s=\left[1-\frac{(1+e^{-2kd})\frac{1}{2}v_F}{\left(Dk+\frac{1}{2}v_F+e^{-2kd}\right)\left(\frac{1}{2}v_F-Dk\right)}\right]\times\frac{g\mu_B}{4\pi M_s}\tilde{g}_{\uparrow\downarrow}\frac{1}{d}, \tag{12}$$

where d is the thickness of NM, $k=1/\delta_{sp}$. In the limit of $d\gg\delta_{sp}$

$$\alpha_{sp}^s=\left[\frac{\sqrt{\epsilon/3}}{\sqrt{\epsilon/3+\frac{1}{2}}}\right]\frac{g\mu_B}{4\pi M_s}\tilde{g}_{\uparrow\downarrow}\frac{1}{d}, \tag{13}$$

where $\epsilon=\tau_m/\tau_{sf}$. Note that the approach to saturation for α_{sp} is proportional to the product of the electron lifetimes ($\delta_{sd}=v_F(\tau_m\tau_{sf}/3)^{1/2}$) while the maximum increase in damping is given by the ratio $\epsilon=\tau_m/\tau_{sf}$.

For a double layer F1/NM/F2 the additional interface spin pumping damping is given by

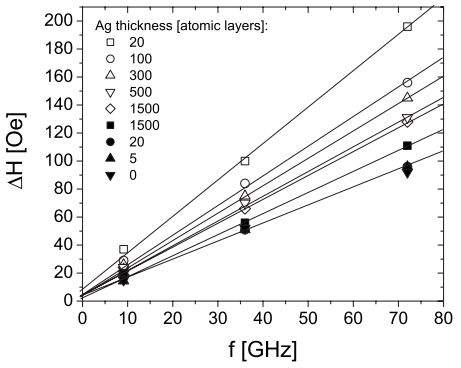

FIG. 1. The FMR linewidth ΔH as a function of the microwave frequency f in the 16 Fe film in GaAs/16 Fe/nAg/12 Fe/20 Au(001) structures (n=20,100, 300,500,1500) are shown by the open symbols. The integers represents the number of atomic layers. The thickness of the Ag spacer is also shown in the inset with appropriate symbols. The solid symbols show the FMR linewidth for the 16 Fe layer in GaAs/16 Fe/mAg/20 Au(001) structures (m=0, 5, 20, and 1500). The thickness of the Ag cover layer is also shown in the inset with appropriate symbols. Notice that the FMR linewidth in Fe/Ag/Fe decreases with an increasing Ag layer thickness; in Fe/Ag/Au it is nearly independent of the Ag layer thickness for m=0, 5, and 20 and becomes noticeably increased for m=1500.

$$\alpha_{sp}^{d} = \left[1 - \frac{\left[\left(Dk + \frac{1}{2}\upsilon_F\right) + e^{-2kd}\left(Dk - \frac{1}{2}\upsilon_F\right)\right]\frac{1}{2}\upsilon_F}{\left(Dk + \frac{1}{2}\upsilon_F\right)^2 - e^{-2kd}\left(Dk - \frac{1}{2}\upsilon_F\right)^2}\right] \times \frac{g\mu_B}{4\pi M_s}\tilde{g}_{\uparrow\downarrow}\frac{1}{d}. \quad (14)$$

Obviously in the limit $d \gg \delta_{sp}$ Eqs. (12) and (14) lead to the same result given in Eq. (13). Notice that the square brackets in Eqs. (12) and (14) are given by τ_m and τ_{sf}, see above. Therefore fitting the data requires us to determine the spin mixing conductance $g_{\uparrow\downarrow}$, bulk Gilbert damping α_b, τ_m, and τ_{sf} parameters. The parameters υ_F (=1.4×10^8 cm/s in Ag), the Landé g factor (=2.09 in Fe), and the saturation magnetization M_s (=1.71×10^3 G in Fe) are well-known constants.

IV. RESULTS

The frequency dependence of the FMR linewidth $\Delta H(f)$ for the 16 Fe layer in GaAs/16 Fe/nAg/12 Fe/20 Au(001) is shown in Fig. 1. FMR measurements in this study were carried out at room temperature (RT). Note that $\Delta H(f)$ is a linear function of the microwave frequency (f) with a small zero frequency offset of 4 Oe. This demonstrates a high quality of MBE grown Fe films with very small presence of extrinsic damping. The average Gilbert damping parameter α was determined from the slope of $\Delta H(f)$ shown in Fig. 1.

Notice that α decreases with an increasing Ag layer thickness. This is expected since the maximum of spin pumping damping is achieved by the second 12 Fe layer which acts as a perfect spin sink (brake). With an increasing Ag layer thickness only a part of the spin accumulated momentum density in Ag reaches the 12 Fe layer and consequently the spin pumping damping becomes increasingly governed by spin relaxation in the Ag spacer which is less effective-spin brake than the Ag/16 Fe interface, see also Eq. (14). The total damping parameter α for the 16 Fe layer in 16 Fe/nAg/12 Fe/20 Au (filled circles) and 16 Fe/mAg/20 Au (open circles) structures as a function of the Ag layer thickness is shown in Fig. 2.

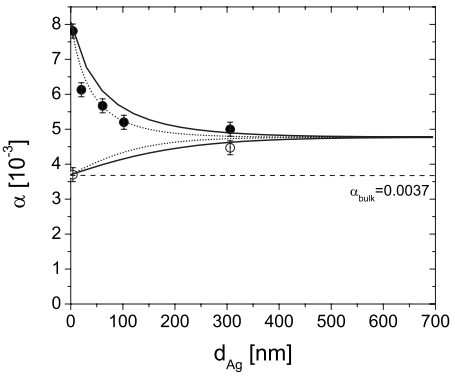

FIG. 2. Thickness dependence of the damping parameter α in 16 Fe as a function of the Ag spacer in GaAs/16Fe/nAg/12 Fe/20 Au(001), see the solid circles, where n=20,100,300,500,1500. The spacing between the atomic layers are 0.145, 0.204, and 0.2045 nm for Fe, Au, and Ag, respectively. The damping parameter was obtained from the slopes of linear fits in Fig. 1. The open circles correspond to the damping in single magnetic layers GaAs/16 Fe/mAg/20 Au(001) with m=20 and 1500. The upper and lower solid lines were obtained by using the parameters obtained in fitting procedure (a), see Table I. The upper dashed line was obtained by fitting the first four solid points [procedure (b)], fitting parameters are listed in Table I. The bottom dashed line was obtained by using Eq. (12) and the parameters employed for fitting the first four solid circles [procedure (b)].

Fitting the data for the magnetic double layers using Eq. (14) required to determine the bulk Gilbert damping α_b and spin mixing conductance $g_{\uparrow\downarrow}$. These two parameters were obtained using the GaAs/16 Fe/20 Ag/20 Au(001) and GaAs/16 Fe/20 Ag/12 Fe/20 Au(001) samples, see Fig. 2. The sample GaAs/16Fe/20Ag/10Au(001), having a decreased thickness of the Au capping layer by a factor of two, had the same FMR linewidth as that in GaAs/16 Fe/20 Ag/20 Au(001). This clearly indicates that in these samples the relaxation of spin momentum inside the Ag and Au layers can be neglected. Therefore the FMR linewidth from the sample GaAs/16 Fe/20 Ag/20 Au(001) allows one to determine the intrinsic bulk Gilbert damping for the 16 Fe film; $\alpha_b=(3.7\pm0.2)\times10^{-3}$. The FMR linewidth in the magnetic double layer GaAs/16 Fe/20 Ag/12 Fe/20 Au(001) sample is then given by adding the contributions from the bulk Gilbert damping α_b and a maximum spin pumping interface damping. The second 12 Fe layer acts as a perfect spin sink for the spin current generated in the 20 Ag spacer. In this case the spin transport with the 20 Ag spacer is simplified, the spin transport is in ballistic limit (unattenuated inside the Ag spacer). The accumulated magnetic moment in the 20 Ag spacer creates two currents. The first current $(-\frac{1}{2}\upsilon_F \boldsymbol{s}_N)$ moves

toward the 16 Fe/20 Ag interface and the second current $(+\frac{1}{2}v_F s_N)$ moves toward the 20 Ag/12 Fe interface, and they are fully absorbed at the Fe/Ag and Ag/Fe interfaces. In this case only half of the pumped spin momentum gets absorbed at the 20 Ag/16 Fe interface and contributes to the FMR linewidth in the 16 Fe layer. In this spin ballistic limit

$$\alpha_{sp} = \frac{g\mu_B}{4\pi M_s} g_{\uparrow\downarrow} \frac{1}{d}, \tag{15}$$

where the Landé g factor and saturation magnetization M_s for Fe is 2.09 and 1.71×10^3 G, respectively. Equation (15) can be also obtained from Eq. (14) for $d\rightarrow 0$. The Fermi velocity in Ag is known to be $v_F=1.4\times10^8$ cm/s. The Gilbert parameter α for the 16 Fe film in GaAs/16 Fe/20 Ag/12 Fe/20 Au(001) after subtraction of α_b resulted [using Eq. (15)] in the spin mixing conductance $g_{\uparrow\downarrow}=1.1\times10^{15}$ cm^{-2}. It is important to note that this measured $g_{\uparrow\downarrow}=1.1\times10^{15}$ cm^{-2} is just slightly below the calculated $g_{\uparrow\downarrow}=1.2\times10^{15}$ cm^{-2} using first-principles electron band calculations[15] carried out at $T=0$.

Analysis of the data by spin-diffusion equation requires a comment. It is strictly valid for Ag spacers significantly thicker than the electron mean free path, ζ. From the Ag bulk conductivity at RT one obtains $\tau_{b,m}=3.7\times10^{-14}$ s and corresponding $\zeta\simeq 50$ nm. Clearly the points for the Ag thickness 21, 61, and 102 nm in Fig. 2 are affected by electron bulk and diffuse scattering at the Fe/Ag/Fe interfaces. The last two data points with the 1500 Ag layer (306 nm) in are already in a fully developed diffuse limit. This is important because this asymptotic limit determines the ratio of the electron relaxation time constants ϵ. The parameter ϵ is a small number in weak spin-orbit interaction systems. In discussions one usually uses its reciprocal value which is described further on by the parameter $\eta=1/\epsilon$. Our analysis were carried out using two fitting procedures.

(a) This fitting procedure used the data points satisfying the spin ballistic and fully spin-diffusion limits. In this case we are limited to the samples GaAs/16 Fe/20 Ag/20 Au, GaAs/16 Fe/20 Ag/12 Fe/20 Au, GaAs/16 Fe/1500 Ag/20 Au, and GaAs/16 Fe/1500 Ag/12 Fe/20 Au. The first two samples allowed one to determine the parameters α_b and $g_{\uparrow\downarrow}$, see above. The ratio $306/50\simeq 6$ assures that the samples with the thick 1500 Ag (306 nm) layer are in a proper spin-diffusion limit where the momentum relaxation time is given mostly by scattering with phonons inside the Ag spacer and little affected by interface diffuse scattering, see the thickness dependence of sheet resistance in Ref. 12. Therefore τ_m is given by the Ag bulk momentum relaxation time at RT, $\tau_{b,m}=3.7\times10^{-14}$ s. In this case one needs to find only τ_{sf} which is required to fit these two data points for $d=300$ nm. All other parameters are known. Analysis of data from Fig. 2 resulted in $\tau_{sf}=3.2\times10^{-12}$ s for the GaAs/16 Fe/1500 Ag/20 Au sample and $\tau_{sf}=1.8\times10^{-12}$ s for GaAs/16 Fe/1500 Ag/12 Fe/20 Au sample. The average value of the spin-flip scattering time, $\bar{\tau}_{sf}=(2.5\pm0.7)\times10^{-12}$ s. The error for τ_{sf} was estimated by taking the standard deviation of the mean. The corresponding parameters $\bar{\eta}=68\pm20$ and spin-diffusion length of $\bar{\delta}_{sd}=245\pm30$ nm. All parameters are listed in Table I. The solid lines shown in Fig. 2 were obtained by employing Eqs. (12) and (14) with the parameters of τ_m and $\bar{\tau}_{sf}=(2.5\pm0.7\times)10^{-12}$ s listed in Table I.

TABLE I. Fitting parameters for the momentum, τ_m, τ_m^{eff}, and spin flip, $\bar{\tau}_{sf}$, τ_{sf}^{eff}, relaxation time constants were obtained by procedure listed in the text under the label (a) and label (b), respectively. The spin-diffusion lengths $\bar{\delta}_{sd}$ and δ_{sd}^{eff} were calculated using Eq. (10). The $\bar{\eta}$ and η_{eff} are given by ratios of $\bar{\tau}_{sf}/\tau_m$ and $\tau_{sf}^{\text{eff}}/\tau_m^{\text{eff}}$ respectively.

Fitting	τ_m	$\bar{\tau}_{sf}$	$\bar{\eta}$	$\bar{\delta}_{sd}$
Procedure (a)	10^{-14} s	10^{-12} s		nm
Solid lines in Fig. 2	3.7 (bulk)	2.5 ± 0.7	68 ± 20	245 ± 30
Fitting	τ_m^{eff}	τ_{sf}^{eff}	η^{eff}	δ_{sd}^{eff}
Procedure (b)	10^{-14} s	10^{-12} s		nm
Dotted lines in Fig. 2	2.4	1.6	67	158

The solid lines fit for the data points with 1500 Ag are within the error bar of FMR measurements. However the upper solid line significantly deviates from the data points in the thickness range where the electron charge and spin transport inside the Ag spacer is neither in ballistic nor spin-diffusion limit (mixed state) and is affected by diffuse scattering at interfaces.

(b) In this fitting procedure the spin-diffusion theory was applied to all data points for the magnetic double layer structures except the last point (1500 Ag spacer). The α_b and $g_{\uparrow\downarrow}$ were determined in the spin ballistic limit (here $d\rightarrow 0$) and are equal to those in approach (a). In this case one carries out two parameter fit for τ_m and τ_{sf}. In this approach one can estimate effective electron-spin transport parameters in the thickness range where the charge and spin transport are in mixed state, neither in fully ballistic nor fully spin-diffusion limits, and affected by diffuse scattering at interfaces. Fitting parameters for τ_m^{eff}, τ_{sf}^{eff}, η^{eff}, and δ_{sd}^{eff} are listed in Table I.

Computer fit to the solid points is shown by the upper dotted line in Fig. 2. The lower dotted line is given by Eq. (12), the fitting parameters are listed in Table I.

V. DISCUSSION OF RESULTS

Notice that the solid lines in Figs. 2 provide a poor fit for intermediate thicknesses. That can be expected because simple diffuse theory does not account properly for nonlocal electron and spin transport. The average electron momentum relaxation time obtained in (b) is about 35% lower than that in the bulk Ag, see Table I. This is reasonable result considering that the ratio of the Ag spacer thickness to the mean free path in bulk Ag is in the range of 1–2. It is interesting to note that the parameters η obtained in (a) and (b) are very close and consequently the spin-diffusion length in (b) is lower than that in (a). Similar measurements using single magnetic GaAs/Fe/Au(001) structures resulted in τ_m by a factor of two smaller than that found in the bulk Au.[9,10] This

can be expected considering that the ratio d/ζ in the Au films was smaller than that in the Ag spacers. The parameter $\eta \simeq 70$ for Ag is significantly larger that that found in Au ($\eta=12$) and the effective spin-diffusion length $\delta_{sd}^{\text{eff}} \simeq 160$ nm is larger than that found in the Au films (=35 nm).[9] This is expected because the atomic number Z of Au (=79) is appreciably larger than that of Ag (=47) and consequently the spin-orbit interaction in Au is appreciably stronger than that in Ag.

It is interesting to compare the electron relaxation time parameters in our thin-film structures with the results obtained by Monod *et al.* using thick Ag and Au crystalline slabs in electron-spin resonance (ESR) experiments.[16] In their case the interfaces played very minor role in electron scattering. However their ESR measurements had to be carried out close to liquid He temperature. The resistivity ratio in their samples reached several thousands. In order to compare their and our results one has to use a parameter that can be in principle weakly dependent on temperature. The parameter $\eta=1/\epsilon=\tau_{sf}/\tau_m$ is possibly the best choice. According to Elliot[8] one expects that in simple metals $\tau_{sf}=\tau_m/(\Delta g)^2$, where Δg is the deviation of the g-factor from the free-electron value. $\Delta g=\xi/\Delta E$, where ξ is the spin-orbit interaction parameter and ΔE is an appropriate difference in energy levels.[17] Since Δg and ΔE are weakly dependent on temperature the parameter η could be expected to have weak dependence on temperature. In our work the mean value of the parameter $\bar{\eta} \simeq 70$ [obtained for thick Ag spacer using fitting procedure (a)] while in the ESR studies $\eta \simeq 400$.[18]

One should emphasize that the best information about the parameter η is obtained in fitting procedure (a) where spin-diffusion theory is valid. In this case the Ag spacer thickness is about a factor of six larger that the mean free path of electron; the sheet resistance even in the presence of diffuse scattering reaches nearly its bulk value.[12] This means that the randomness in electron momentum distribution is already governed by scattering with phonons thermally excited inside the Ag spacer. Therefore it is quite possible that the lower value for η in our measurements compared to that in ESR is caused by intrinsic mechanism. One should realize that the ESR measurements had to be carried out at cryogenic temperatures well below the Debye temperature (T_D), while our RT measurements were carried out well above T_D. This suggests that the spin-flip relaxation rate is significantly enhanced by scattering of electrons with thermally excited phonons having q wave vectors across a whole Brillouin zone.

Surprising result for the parameter η was found in the study by Godfrey and Johnson[3] using a lateral spin valve Py/Ag mesoscopic wire/Py structure. The spin-diffusion length at RT in their study was 140 nm which is smaller than in our studies, 245 nm. However it is interesting to note that their samples have significantly increased resistivity by a factor 3.4 and 2.6 compared to those in fitting procedures (a) and (b), respectively. Surprisingly their $\tau_{sf}=2.6\times10^{-12}$ s is very close to that found in our studies in pure spin-diffusion limit [fitting procedure (a)], $\bar{\tau}_{sf}=2.5\times10^{-12}$ s. In fact their appreciable larger value of $\eta \simeq 240$ was caused by a significantly smaller momentum relaxation parameter in the lateral spin valves when compared to our results. This would imply that a strong defect scattering in their Ag wires contributed only weakly to spin-flip scattering. This is indeed surprising result considering that nonlocal spin valves have more complicated geometry with bigger surface area for interface scattering (compared to our planar geometry) and include grain boundaries in polycrystalline Ag.

VI. CONCLUSIONS

Spin transport in magnetic double GaAs/Fe/Ag/Fe/Au(001) and single GaAs/Fe/Ag/Au(001) layer structures was investigated by spin pumping effect using FMR linewidth as a function of the Ag spacer. The results were interpreted by using magnetoelectronics circuits and Kirchhoff's laws and spin-diffusion equations inside the Ag spacers. The spin mixing conductance had to be enhanced by subtracting the Sharvin conductance which justifies the use of Kirchhoff's laws in our studies. Four parameters were required to fit the FMR data; the bulk damping α_b in Fe, spin mixing conductance $g_{\uparrow\downarrow}$, spin momentum relaxation time τ_m, and spin-flip relaxation time τ_{sf}. α_b and $g_{\uparrow\downarrow}$ were determined from the magnetic single and double Fe layer samples satisfying the ballistic spin momentum transport. The relaxation times were determined by two fitting procedures: (a) the spin transport satisfied fully spin-diffusion limit; electron charge and spin relaxation are governed by scattering with phonons inside the spacer. (b) Spin-diffusion theory was applied to an intermediate range of thicknesses allowing one to determine effective electron scattering time parameters. In this case the electron charge and spin transport is in a mixed state; only partly ballistic and affected by diffuse scattering at interfaces.

The following fitting parameters were found: $\alpha_b=0,0037$, $g_{\uparrow\downarrow}=1.1\times10^{15}$ cm^{-2}. (a) The momentum relaxation time $\tau_m=3.7\times10^{-14}$ s (bulk Ag), spin-flip relaxation time $\bar{\tau}_{sf}=2.5\pm0.7\times10^{-12}$ s, the corresponding spin-diffusion length $\bar{\delta}_{sd}=245\pm30$ nm, and the ratio of relaxation time parameters $\bar{\eta}=68\pm20$. (b) $\tau_m^{\text{eff}}=2.4\times10^{-14}$ s, $\tau_{sf}^{\text{eff}}=1.6\times10^{-12}$ s, $\delta_{sd}^{\text{eff}}=158$ nm, and the ratio of relaxation-time parameter $\eta^{\text{eff}}=67$. These results were compared and discussed with the results obtained in the bulk Ag slabs carried out at cryogenic temperatures and with the nonlocal Ag spin valves. It is argued that a significant decrease in the parameter η (by a factor 5) in our FMR studies carried out at RT compared to those performed using ESR technique at cryogenic temperatures can be caused by a significantly enhanced spin-flip scattering by phonons at RT. Surprising differences between the results in our and the lateral spin valve (nanoscopic systems) studies beg for formulating a full nonlocal spin transport theory allowing one to account properly for the spin-dependent phonon, impurity, grain boundary, and interface scattering.

ACKNOWLEDGMENTS

Financial support from the Natural Sciences and Engineering Research Council of Canada (NSERC) and the Canadian Institute for Advanced Research (CIAR) is gratefully acknowledged.

*bkardasz@sfu.ca

[1] Y. Ji, A. Hoffmann, J. Pearson, and S. Bader, Appl. Phys. Lett. **85**, 6218 (2004).
[2] J. Laloe, T. Yang, T. Kimura, and Y. Otani, J. Appl. Phys. **105**, 07D110 (2009).
[3] R. Godfrey and M. Johnson, Phys. Rev. Lett. **96**, 136601 (2006).
[4] T. Kimura, Y. Otani, T. Sato, S. Takahashi, and S. Maekawa, Phys. Rev. Lett. **98**, 156601 (2007).
[5] Y. Tserkovnyak, A. Brataas, G. Bauer, and B. Halperin, Rev. Mod. Phys. **77**, 1375 (2005).
[6] Y. Tserkovnyak, A. Brataas, and G. E. W. Bauer, Phys. Rev. Lett. **88**, 117601 (2002).
[7] B. Heinrich, Y. Tserkovnyak, G. Woltersdorf, A. Brataas, R. Urban, and G. E. W. Bauer, Phys. Rev. Lett. **90**, 187601 (2003).
[8] R. J. Elliott, Phys. Rev. **96**, 266 (1954).
[9] B. Kardasz, O. Mosendz, B. Heinrich, Z. Liu, and M. Freeman, J. Appl. Phys **103**, 07C509 (2008).
[10] O. Mosendz, G. Woltersdorf, B. Kardasz, B. Heinrich, and C. H. Back, Phys. Rev. B **79**, 224412 (2009).
[11] A. Brataas, G. Bauer, and P. Kelly, Phys. Rep. **427**, 157 (2006).
[12] T. L. Monchesky, A. Enders, R. Urban, K. Myrtle, B. Heinrich, X.-G. Zhang, W. H. Butler, and J. Kirschner, Phys. Rev. B **71**, 214440 (2005).
[13] B. Heinrich, *Magnetic Ultrathin Film Structures III*, edited by J. A. C. Bland and B. Heinrich (Springer, New York, 2004), Chap. 5, p. 143.
[14] B. Heinrich and J. F. Cochran, Adv. Phys. **42**, 523 (1993).
[15] M. Zwierzycki, Y. Tserkovnyak, P. J. Kelly, A. Brataas, and G. E. W. Bauer, Phys. Rev. B **71**, 064420 (2005).
[16] P. Monod and F. Beuneu, Phys. Rev. B **19**, 911 (1979).
[17] Y. Yafet, *Solid State Physics*, edited by F. Seitz and D. Turnbull (Academic Press, New York, 1963), Vol. 14, p. 1.
[18] F. Beuneu and P. Monod, Phys. Rev. B **18**, 2422 (1978).